ISSN 1063-7834, Physics of the Solid State, 2021, Vol. 63, No. 1, pp. 113–121. © Pleiades Publishing, Ltd., 2021, corrected publication 2021.
Russian Text © The Author(s), 2021, published in Fizika Tverdogo Tela, 2021, Vol. 63, No. 1, pp. 111–119

OPTICAL PROPERTIES

Comparison of the Absorption Spectra of Nd^{3+} Ions in the $NdFe_3(BO_3)_4$, $Nd_{0.5}Gd_{0.5}Fe_3(BO_3)_4$, and $Ho_{0.75}Nd_{0.25}Fe_3(BO_3)_4$ Crystals

A. L. Sukhachev[a, *], A. V. Malakhovskii[a], C. S. Nelson[b], I. A. Gudim[a], and V. L. Temerov[a]

[a] *Kirensky Institute of Physics, FRC KSC SB RAS, Krasnoyarsk, 660036 Russia*
[b] *National Synchrotron Light Source II, Brookhaven National Laboratory, Upton, N.Y., 11973 USA*
**e-mail: sunya@iph.krasn.ru*

Received September 2, 2020; revised September 2, 2020; accepted September 2, 2020

Abstract—The polarized optical absorption spectra in the region of a series of the *f–f* transitions of Nd^{3+} ions in the $Ho_{0.75}Nd_{0.25}Fe_3(BO_3)_4$, $Nd_{0.5}Gd_{0.5}Fe_3(BO_3)_4$, and $NdFe_3(BO_3)_4$ crystals at 90 K have been compared. The spectral features related to the difference in the local environment of Nd^{3+} ions in these crystals have been established. In the region of the transition ${}^4I_{9/2} \rightarrow {}^4G_{5/2} + {}^2G_{7/2}$ of Nd^{3+} ions in the $Ho_{0.75}Nd_{0.25}Fe_3(BO_3)_4$ crystal, the appearance of some absorption lines at the structural transition $R32 \rightarrow P3_121$ around ~200 K due to the local symmetry variation has been found. The intensity of these lines smoothly increases with a decrease in temperature from the transition point. The temperature dependence of the lattice parameters of the $Ho_{0.75}Nd_{0.25}Fe_3(BO_3)_4$ crystal has been measured. It has been found that, at the transition temperature, the lattice parameter *a* changes stepwise, which is indicative of the occurrence of a first-order phase transition. The lattice parameter *c* changes smoothly.

Keywords: neodymium, hantite-structure ferroborates, *f–f* electronic transitions, structural transition
DOI: 10.1134/S1063783421010200

1. INTRODUCTION

Ferroborates $RFe_3(BO_3)_4$, where R is Y or a rare-earth (RE) element, have a hantite-like structure. The RE ferroborates attract great attention of researchers because such crystals are often multiferroics [1–3]. The $NdFe_3(BO_3)_4$, $Nd_{0.5}Gd_{0.5}Fe_3(BO_3)_4$, and $Ho_{0.75}Nd_{0.25}Fe_3(BO_3)_4$ crystals investigated here belong to the materials of this type, as was demonstrated by studying their magnetic, magnetoelastic, and magnetoelectric properties [3–5]. The combination of the physical characteristics and chemical stability of borates with a hantite structure allows them to be used in optical and optoelectronic devices [6–8], in particular, for adding and multiplying laser radiation frequencies [9, 10].

The optical properties of RE ions, specifically, the *f–f* transitions, are determined by the symmetry of the local environment of an ion. At high temperatures, RE ferroborates crystallize in a trigonal structure (sp. gr. *R*32) [10–14]. The unit cell contains three formula units. Rare-earth ions are located at the centers of RO_6 trigonal prisms with the D_3 local symmetry. Fe^{3+} ions occupy sites with the C_3 symmetry in oxygen octahedra. These octahedra form helicoidal chains along the crystallographic C_3 axis. As the temperature decreases, some RE ferroborates with small radii of the RE ion undergo a structural transition to the phase with sp. gr. $P3_121$ [10–12]. This leads to a decrease in the local symmetry of the RE ion to C_2 and the occurrence of two nonequivalent sites of Fe^{3+} ions. As was shown in the study of the Raman scattering spectra in the $Ho_{0.75}Nd_{0.25}Fe_3(BO_3)_4$ crystal in the temperature range of 10–400 K [15], at a temperature of 203 K, the displacement-type structural transition $R32 \rightarrow P3_121$ occurs.

In [16], the optical absorption spectra were examined and the electronic structure of Nd^{3+} ions in the $NdFe_3(BO_3)_4$ crystal at a temperature of 50 K was established. In [17], the electronic structure of Nd^{3+} ions in the $Nd_{0.5}Gd_{0.5}Fe_3(BO_3)_4$ crystal at a temperature of 40 K was determined using the analysis of the polarized optical absorption and magnetic circular dichroism spectra. According to the data reported in [16, 17], the *R*32 spatial symmetry of the $NdFe_3(BO_3)_4$ and $Nd_{0.5}Gd_{0.5}Fe_3(BO_3)_4$ crystals is retained to helium temperatures. The room-temperature optical absorption spectra and the Judd–Ofelt parameters for the $Nd_{0.5}Gd_{0.5}Fe_3(BO_3)_4$ crystal [18] and the

$NdFe_3(BO_3)_4$ and $Ho_{0.75}Nd_{0.25}Fe_3(BO_3)_4$ crystals [19] were obtained.

In this study, we carry out a comparative study of the absorption spectra of Nd^{3+} ions in $NdFe_3(BO_3)_4$, $Nd_{0.5}Gd_{0.5}Fe_3(BO_3)_4$, and $Ho_{0.75}Nd_{0.25}Fe_3(BO_3)_4$ crystals in order to elucidate the effect of local symmetry of the Nd^{3+} ion and weaker lattice distortions caused by the replacement of the Nd^{3+} ion by other RE ions.

2. EXPERIMENTAL

The crystals to be investigated were grown using a flux technique. The $Nd_{0.5}Gd_{0.5}Fe_3(BO_3)_4$ single crystals were grown from the $K_2Mo_3O_{10}$-based flux using the procedure described in [18, 20]. The $Ho_{0.75}Nd_{0.25}Fe_3(BO_3)_4$ and $NdFe_3(BO_3)_4$ crystals were grown from the $Bi_2Mo_3O_{12}$-based flux [19, 21]. The stoichiometric composition of the grown crystals was determined from the ratio of the RE oxides used in the synthesis. The samples for measurements were ~0.2-mm-thick plates with the crystallographic C_3 axis lying in the sample plane.

The absorption spectra were recorded on an automated double-beam spectrophotometer based on an MDR-2 monochromator. The optical slit width during the spectral measurements was 0.2 nm in the range of 500–600 nm and 0.4 nm in the range of 600–1000 nm. The samples were cooled in a nitrogen gas continuous-flow cryostat. The temperature was maintained with an accuracy of ~1 K. The absorption spectra were measured during propagation of the linearly polarized light along the normal to the C_3 crystal axis at the light wave vector **E** parallel (π polarization) and perpendicular (σ polarization) to the crystal C_3 axis.

X-ray scattering measurements were carried out using a 4-circle diffractometer in a vertical scattering geometry at wiggler beamline X21 at Brookhaven National Laboratory's National Synchrotron Light Source. The lattice parameters were determined by measuring the (600) and (006) Bragg peaks as a function of temperature at a photon energy of 10 keV and with a LiF(200) analyzer crystal.

3. RESULTS AND DISCUSSION

The optical absorption spectra of the $Ho_{0.75}Nd_{0.25}Fe_3(BO_3)_4$, $Nd_{0.5}Gd_{0.5}Fe_3(BO_3)_4$, and $NdFe_3(BO_3)_4$ crystals were measured at $T = 90$ K in the π and σ polarizations. Figure 1 shows the absorption spectra of the $Ho_{0.75}Nd_{0.25}Fe_3(BO_3)_4$ crystal. The spectra contain broad bands corresponding to the *d–d* transitions in Fe^{3+} ions and narrow lines of the *f–f* transitions in Nd^{3+} and Ho^{3+} ions. The *d–d* absorption bands of Fe^{3+} ions were subtracted from the total spectra. The absorption coefficients were reduced to the molar concentration of Nd^{3+} ions. The Nd^{3+} ion concentration in the $NdFe_3(BO_3)_4$ crystal is

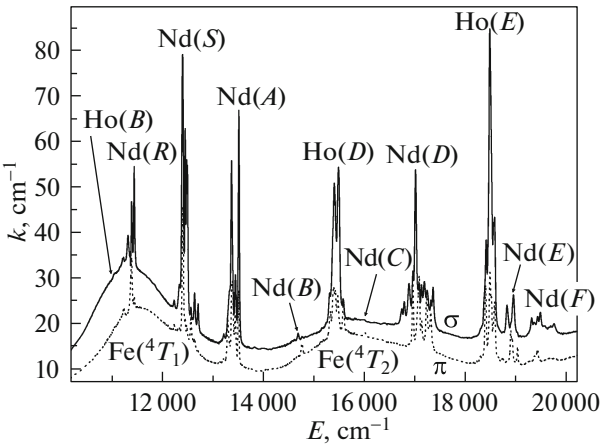

Fig. 1. Optical absorption spectra for the $Ho_{0.75}Nd_{0.25}Fe_3(BO_3)_4$ crystal at $T = 90$ K in the π and σ polarizations.

8.34 mol/L. In the $Nd_{0.5}Gd_{0.5}Fe_3(BO_3)_4$ and $Ho_{0.75}Nd_{0.25}Fe_3(BO_3)_4$ crystals, we have $C_{Nd} = 4.17$ and 2.085 mol/L, respectively [19].

The spatial symmetry of the $NdFe_3(BO_3)_4$ and $Nd_{0.5}Gd_{0.5}Fe_3(BO_3)_4$ crystals at 90 K is *R*32. The local symmetry of Nd^{3+} ions is D_3. For ions with a half-integer moment in the D_3 symmetry, there are the states of two types: $E_{1/2}$ and $E_{3/2}$. The states of a free atom with half-integer total moment *J* split in a cubic crystal field and, then, in a D_3 symmetry field as

$$J = 3/2 \to G_{3/2} \to E_{1/2} + E_{3/2}, \quad (1)$$

$$J = 5/2 \to E_{3/2} + G_{3/2} \to E_{1/2} + (E_{1/2} + E_{3/2}), \quad (2)$$

$$J = 7/2 \to E_{1/2} + E_{3/2} + G_{3/2} \to E_{1/2} + E_{1/2} + (E_{1/2} + E_{3/2}), \quad (3)$$

$$J = 9/2 \to E_{1/2} + 2G_{3/2} \to E_{1/2} + 2(E_{1/2} + E_{3/2}). \quad (4)$$

At the D_3 symmetry of the local environment of a RE ion, the electric dipole transitions between the states occur according to the selection rules (Table 1). As was shown in [16, 17], all the investigated transitions are electric dipole. When the symmetry of the local environment changes from D_3 to C_2, the difference between the states $E_{1/2}$ and $E_{3/2}$ vanishes and the transitions become allowed in both the π and σ polarizations. This is observed in the investigated $Ho_{0.75}Nd_{0.25}Fe_3(BO_3)_4$ crystal, since its spatial sym-

Table 1. Selection rules for the electric dipole transitions in the D_3 symmetry

	$E_{1/2}$	$E_{3/2}$
$E_{1/2}$	π, σ(*a*)	σ(*a*)
$E_{3/2}$	σ(*a*)	π

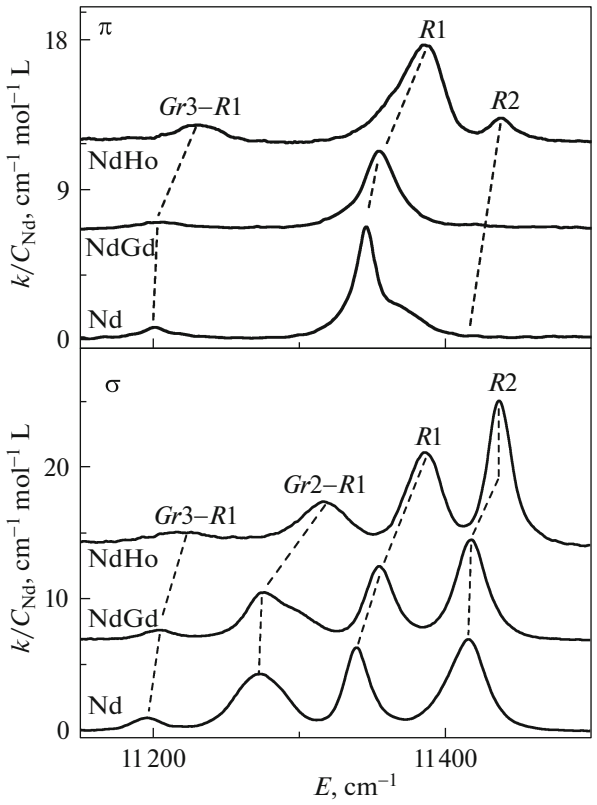

Fig. 2. Absorption spectra of the transition $^4I_{9/2} \rightarrow {}^4F_{3/2}$ (R) of Nd^{3+} ions in the π and σ polarizations for the $Ho_{0.75}Nd_{0.25}Fe_3(BO_3)_4$ (NdHo), $Nd_{0.5}Gd_{0.5}Fe_3(BO_3)_4$ (NdGd), and $NdFe_3(BO_3)_4$ (Nd) crystals at $T = 90$ K.

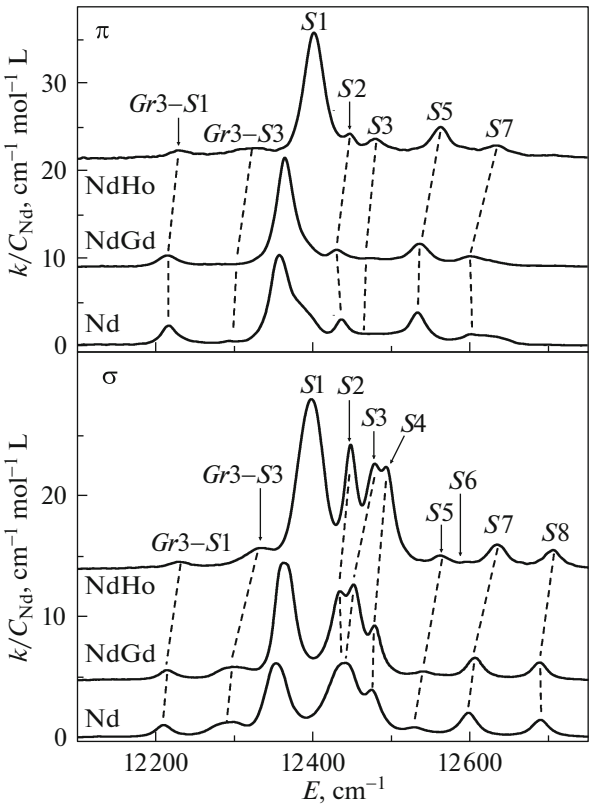

Fig. 3. Absorption spectra of the transition $^4I_{9/2} \rightarrow {}^4F_{5/2} + {}^2H_{9/2}$ (S) of Nd^{3+} ions in the π and σ polarizations for the $Ho_{0.75}Nd_{0.25}Fe_3(BO_3)_4$ (NdHo), $Nd_{0.5}Gd_{0.5}Fe_3(BO_3)_4$ (NdGd), and $NdFe_3(BO_3)_4$ (Nd) crystals at $T = 90$ K.

metry at temperatures below 203 K is $P3_121$ [15] and the local symmetry of the environment of RE ions is C_2. The number of lines (1–4) does not change upon this local symmetry lowering, since in the D_3 symmetry the Nd^{3+} ion states are already split to doublets by the crystal field. The interpretation of the absorption bands and identification of lines of the *f–f* transition of Nd^{3+} ions in the $NdFe_3(BO_3)_4$ and $Ho_{0.75}Nd_{0.25}Fe_3(BO_3)_4$ crystals were performed by comparing with the spectra of the $Nd_{0.5}Gd_{0.5}Fe_3(BO_3)_4$ crystal [17].

Splittings ΔE of the electron multiplets of Nd^{3+} ions in the crystal field obtained from the experimental data are given in Table 2. The difference between the level splitting in the investigated crystals points out the difference between the even crystal field components in the region of the Nd^{3+} ion in these crystals. In particular, in most excited multiplets, the splitting ΔE increases in the sequence $Ho_{0.75}Nd_{0.25}Fe_3(BO_3)_4$, $Nd_{0.5}Gd_{0.5}Fe_3(BO_3)_4$, and $NdFe_3(BO_3)_4$. The absorption spectra (Figs. 2–6) show a relative broadening of absorption lines in the $Ho_{0.75}Nd_{0.25}Fe_3(BO_3)_4$ and $Nd_{0.5}Gd_{0.5}Fe_3(BO_3)_4$ crystals as compared with $NdFe_3(BO_3)_4$, which is apparently due to the inhomogeneity of the local environment of Nd^{3+} ions.

The integral intensities of the *f–f* transitions of Nd^{3+} ions in the investigated crystals at a temperature of 90 K are given in Table. 3. They were obtained by integrating the π- and σ-polarized absorption bands (Figs. 2–6) and the subsequent averaging of the intensities according to the relation for uniaxial anisotropic crystals in the form $(2I_\sigma + I_\pi)/3$. At 90 K, in the $Ho_{0.75}Nd_{0.25}Fe_3(BO_3)_4$ crystal, the local symmetry of Nd^{3+} ions is C_2 and the integrated intensity of a sum of all the transitions is noticeably higher than in the other crystals under study, in which the local symmetry is D_3 (Table 3). The higher intensity of the transitions corresponds to the larger odd crystal field component, due to which the *f–f* transitions become resolved.

Transition $^4I_{9/2} \rightarrow {}^4F_{3/2}$ (R band). Figure 2 shows the absorption spectra of the crystals under study in the region of the R ($^4I_{9/2} \rightarrow {}^4F_{3/2}$) transition of Nd^{3+} ions at $T = 90$ K. Lines $R1$ and $R2$ are identified as transitions from the lower component of the splitting of the ground state ($Gr1$); the positions of levels $R1$ and $R2$ are given in Table 2. The line $Gr3–R1$ corresponds to

Table 2. Positions of the energy levels of Nd^{3+} ions in the $Ho_{0.75}Nd_{0.25}Fe_3(BO_3)_4$, $Nd_{0.5}Gd_{0.5}Fe_3(BO_3)_4$, and $NdFe_3(BO_3)_4$ crystals at $T = 90$ K

State	Transition (Level)	$Ho_{0.75}Nd_{0.25}Fe_3(BO_3)_4$ E, cm^{-1}	$Nd_{0.5}Gd_{0.5}Fe_3(BO_3)_4$ E, cm^{-1}	$NdFe_3(BO_3)_4$ E, cm^{-1}	State in the D_3 symmetry [17]
$^4I_{9/2}$	*Gr*1	0	0	0	$E_{1/2}$
	*Gr*2	75	79	71	$E_{3/2}$
	*Gr*3	161	148	143	$E_{1/2}$
	*Gr*4	216	219	219	$E_{1/2}$
	*Gr*5	345	327	321	$E_{3/2}$
$^4F_{3/2}$	*Gr*3–*R*1	11227	11205	11196	
	*Gr*2–*R*1	11318	11276	11272	
	*R*1	11386	11355	11342	$E_{1/2}$
	*R*2	11437	11418	11416	$E_{3/2}$
	ΔE_R	51	63	74	
$^4F_{5/2} + {}^2H_{9/2}$	*Gr*3–*S*1	12228	12215	12212	
	*S*1	12399	12363	12354	$E_{1/2}$
	*S*2	12447	12431	12436	$E_{1/2}$
	*S*3	12477	12451	~12450	$E_{3/2}$
	*S*4	12493	12477	12474	$E_{1/2}$
	*S*5	12562	12537	12531	$E_{1/2}$
	*S*6	–	–	–	$E_{3/2}$
	*S*7	12633	12604	12597	$E_{1/2}$
	*S*8	12704	12687	12688	$E_{3/2}$
	ΔE_S	305	324	334	
$^4F_{7/2} + {}^4S_{3/2}$	*Gr*3–*A*1	13211	13190	13182	
	*A*1	13365	13335	13324	$E_{1/2}$
	*A*2	13385	13350	13340	$E_{3/2}$
	*A*3	~13436	~13403	~13408	$E_{1/2}$
	*A*4	~13442	~13412	~13414	$E_{1/2}$
	*A*5	~13503	13472	13470	$E_{1/2}$
	*A*6	~13510	~13481	~13475	$E_{3/2}$
	ΔE_A	145	146	151	
$^4G_{5/2} + {}^2G_{7/2}$	*Gr*4–*D*1	16740	16711	16704	
	*Gr*5–*D*3	16785	16780	16784	
	*Gr*2–*D*1	16878	16850	16849	
	*D*1	16956	16930	16923	$E_{1/2}$
	*Gr*2–*D*2	17009	16992	16996	
	*Gr*2–*D*3	17051	17028	17030	
	*D*2	17082	17070	17065	$E_{1/2}$
	*D*3	17130	17107	17105	$E_{3/2}$
	*D*4	17227	17208	17205	$E_{1/2}$
	*D*5	17274	17250	17252	$E_{1/2}$
	*D*6	17313	17297	17297	$E_{1/2}$
	*D*7	17356	17335	17332	$E_{3/2}$
	ΔE_D	400	405	409	
$^4G_{9/2}$	*Gr*3–*E*1	18733	18724	18726	
	*Gr*2–*E*1	18819	18792	18796	
	*E*1	18894	18873	18867	$E_{1/2}$
	*E*2	18924	18908	18904	$E_{1/2}$
	*E*3	~18951	18954	~18952	$E_{3/2}$
	*E*4	19026	19011	19010	$E_{1/2}$
	*E*5	19077	19065	19065	$E_{3/2}$
	ΔE_E	183	192	198	

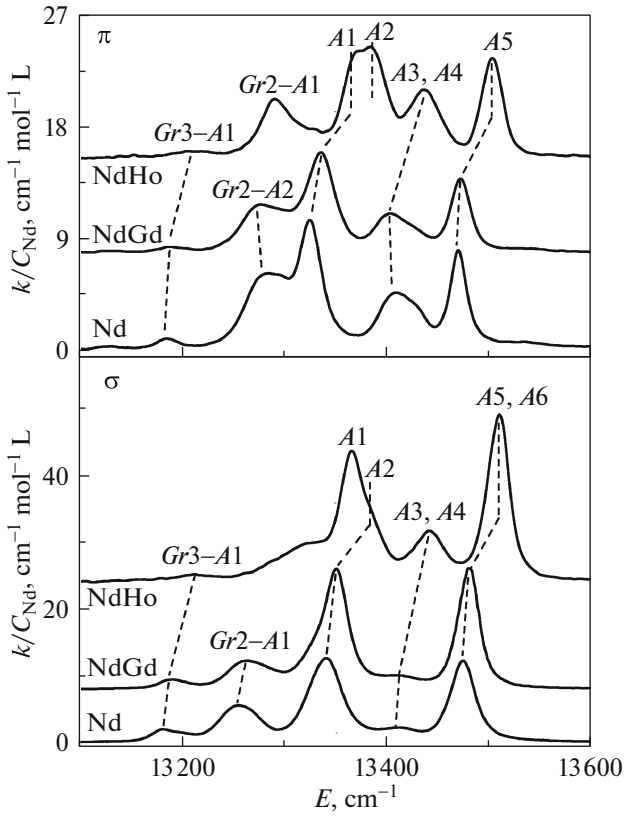

Fig. 4. Absorption spectra of the transition $^4I_{9/2} \rightarrow {}^4F_{7/2} + {}^4S_{3/2}$ (A) of Nd^{3+} ions in the π and σ polarizations for the $Ho_{0.75}Nd_{0.25}Fe_3(BO_3)_4$ (NdHo), $Nd_{0.5}Gd_{0.5}Fe_3(BO_3)_4$ (NdGd), and $NdFe_3(BO_3)_4$ (Nd) crystals at $T = 90$ K.

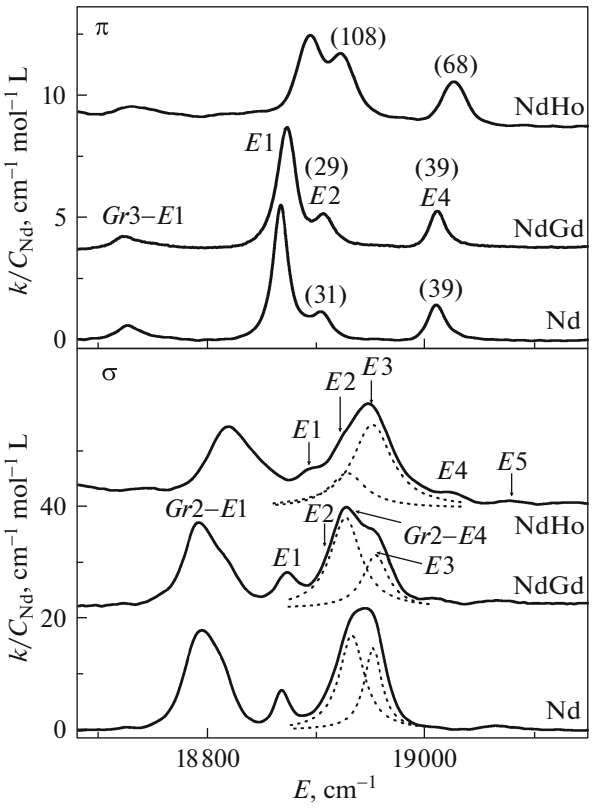

Fig. 5. Absorption spectra of the transition $^4I_{9/2} \rightarrow {}^4G_{9/2}$ (E) of Nd^{3+} ions in the π and σ polarizations for the $Ho_{0.75}Nd_{0.25}Fe_3(BO_3)_4$ (NdHo), $Nd_{0.5}Gd_{0.5}Fe_3(BO_3)_4$ (NdGd), and $NdFe_3(BO_3)_4$ (Nd) crystals at $T = 90$ K. In the π spectra in the parenthesis, the intensities of lines $E2$ and $E4$ (cm^{-2} mol^{-1} L) are indicated which were obtained by the decomposition of the spectra into components of the Lorentzian shape.

the transition from the $Gr3$ sublevel of the ground state to the $R1$ level and the line $Gr2-R1$, to the transition from $Gr2$ to $R1$. Based on this, we obtain the position of components of splitting of the ground state $Gr2$ and $Gr3$ of Nd^{3+} ions in the investigated crystals (Table 2). The energies of the components of splitting of the ground state $^4I_{9/2}$ given in Table 2 were determined by averaging the values obtained from the positions of the corresponding transitions from Table 2. The symmetries of the components of splitting of the ground state $Gr1$, $Gr2$, and $Gr3$ were determined in [17] (see Table 2). The $R2$ transition is forbidden in the π polarization by the selection rules in the D_3 local symmetry (Table 1), while in the $Ho_{0.75}Nd_{0.25}Fe_3(BO_3)_4$ crystal, there is line $R2$ in the π-polarized absorption spectrum (Fig. 2). This follows from the C_2 local symmetry of Nd^{3+} ions in this crystal at 90 K. The relative energy shift of the analogous absorption lines in the crystals under study (Fig. 2) suggests the difference between even crystal field components in the region of Nd^{3+} ions.

Transition $^4I_{9/2} \rightarrow {}^4F_{5/2} + {}^2H_{9/2}$ (S band). The absorption spectra in the region of the S ($^4I_{9/2} \rightarrow {}^4F_{5/2} + {}^2H_{9/2}$) transition are shown in Fig. 3. The $S6$ line, which was observed in [17] at 6 K, is detected at a temperature of 90 K in none of the crystals. The positions of the components of splitting of the states $^4F_{5/2}$ and $^2H_{9/2}$ are given in Table 2. The $S3$ band forbidden by the selection rules in the D_3 symmetry in the π polarization is observed in the absorption spectrum of the $Ho_{0.75}Nd_{0.25}Fe_3(BO_3)_4$ crystal (Fig. 3), where neodymium is in the C_2 position. Line $Gr3-S3$ behaves similarly. Consequently, the $Gr3$ state has the $E_{1/2}$ symmetry (Tables 1 and 2).

Transition $^4I_{9/2} \rightarrow {}^4F_{7/2} + {}^4S_{3/2}$ (A band). Figure 4 shows the absorption spectra in the region of the A ($^4I_{9/2} \rightarrow {}^4F_{7/2} + {}^4S_{3/2}$) transition. In the $NdFe_3(BO_3)_4$ and $Nd_{0.5}Gd_{0.5}Fe_3(BO_3)_4$ crystals, line pairs ($A1$, $A2$), ($A3$, $A4$), and ($A5$, $A6$) are almost indistinguishable. However, in the $Ho_{0.75}Nd_{0.25}Fe_3(BO_3)_4$ crystal, the pair ($A1$, $A2$) is split and both lines become active in the π polarization.

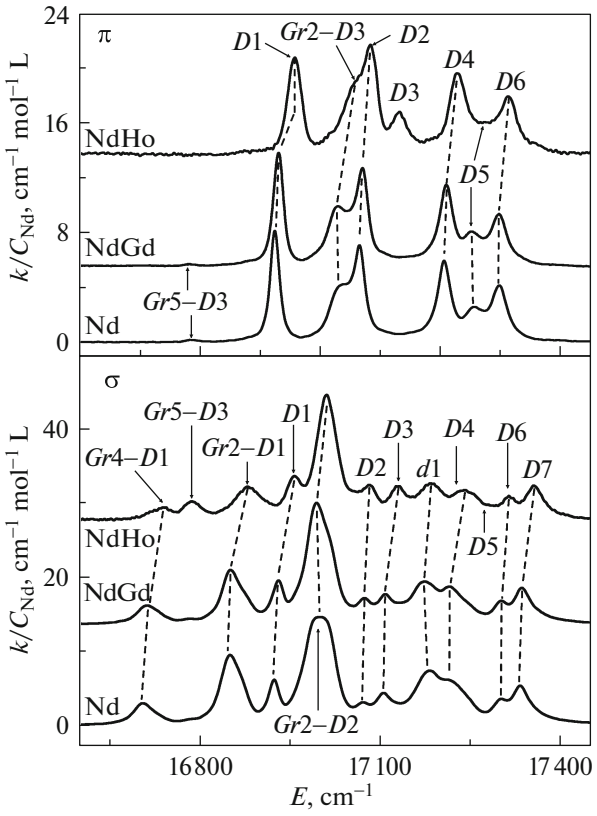

Fig. 6. Absorption spectra of the transition ${}^4I_{9/2} \rightarrow {}^4G_{5/2} + {}^4G_{7/2}$ (D) of Nd^{3+} ions in the π and σ polarizations for the $Ho_{0.75}Nd_{0.25}Fe_3(BO_3)_4$ (NdHo), $Nd_{0.5}Gd_{0.5}Fe_3(BO_3)_4$ (NdGd), and $NdFe_3(BO_3)_4$ (Nd) crystals at $T = 90$ K.

It should be noted that lines $A3$ and $A4$ in the σ-polarized absorption spectrum of the $Ho_{0.75}Nd_{0.25}Fe_3(BO_3)_4$ crystal are much more intense than in the $NdFe_3(BO_3)_4$ and $Nd_{0.5}Gd_{0.5}Fe_3(BO_3)_4$ crystals (Fig. 4). The parity-forbidden f–f transitions are allowed due to the odd crystal field components. Consequently, such a difference between the absorption intensities can be explained by the larger value of the odd crystal field component in the $Ho_{0.75}Nd_{0.25}Fe_3(BO_3)_4$ crystal.

Transition ${}^4I_{9/2} \rightarrow {}^4G_{9/2}$ (E band). In the E (${}^4I_{9/2} \rightarrow {}^4G_{9/2}$) transition (Fig. 5), line $E3$ in the D_3 symmetry is forbidden in the π polarization, but it is not observed in the $Ho_{0.75}Nd_{0.25}Fe_3(BO_3)_4$ crystal either. Note a significant increase in the intensities of lines $E2$ and $E4$ in the π-polarized absorption spectrum of the $Ho_{0.75}Nd_{0.25}Fe_3(BO_3)_4$ crystal (Fig. 5) (the line intensities are shown in the figure). This can be attributed to the greater noncentrosymmetricity of the local environment of the Nd^{3+} ion in this crystal in this electronic state.

Transition ${}^4I_{9/2} \rightarrow {}^4G_{5/2} + {}^2G_{7/2}$ (D band). The absorption spectra in the region of the D (${}^4I_{9/2} \rightarrow {}^4G_{5/2} + {}^2G_{7/2}$) transition of Nd^{3+} ions in the investigated crystals at 90 K are shown in Fig. 6. The positions of the components of splitting of the excited states ${}^4G_{5/2}$ and ${}^2G_{7/2}$ are given in Table 2. The $D5$ transition in the $Ho_{0.75}Nd_{0.25}Fe_3(BO_3)_4$ crystal is very weak in both the π and σ spectrum (Fig. 6); therefore, its position was determined by the factorization of the π spectrum into Lorentzian components. Line $d1$ can be interpreted as either the $Gr2$–$D5$ or $Gr3$–$D7$ transition. The $D3$ transition is forbidden in the π polarization in the D_3 symmetry by the selection rules (Table 1), but in the $Ho_{0.75}Nd_{0.25}Fe_3(BO_3)_4$ crystal, it is clearly seen in the π spectrum (Fig. 6), which follows from the local C_2 symmetry of neodymium ions in this crystal at 90 K.

Table 3. Integral intensities of the f–f transitions ($(2I_\sigma + I_\pi)/3$) in Nd^{3+} ions in the $Ho_{0.75}Nd_{0.25}Fe_3(BO_3)_4$, $Nd_{0.5}Gd_{0.5}Fe_3(BO_3)_4$, and $NdFe_3(BO_3)_4$ crystals at $T = 90$ K

Transition	${}^4I_{9/2} \downarrow$	E, cm^{-1}	$(2I_\sigma + I_\pi)/3$, $cm^{-2}\,mol^{-1}\,L$		
			$Ho_{0.75}Nd_{0.25}Fe_3(BO_3)_4$ $P3_121$ (C_2)	$Nd_{0.5}Gd_{0.5}Fe_3(BO_3)_4$ $R32$ (D_3)	$NdFe_3(BO_3)_4$ $R32$ (D_3)
R	${}^4F_{3/2}$	11350	601	448	516
S	${}^4F_{5/2} + {}^2H_{9/2}$	12400	2331	1618	1540
A	${}^4F_{7/2} + {}^4S_{3/2}$	13350	1888	1297	1439
B	${}^4F_{9/2}$	14600	131	67	87
D	${}^2G_{7/2} + {}^4G_{5/2}$	17000	2188	2046	2412
E	${}^4G_{9/2}$	18900	399	390	436
F	${}^2K_{13/2} + {}^4G_{7/2}$	19400	491	450	506
	Σ		8028	6315	6936

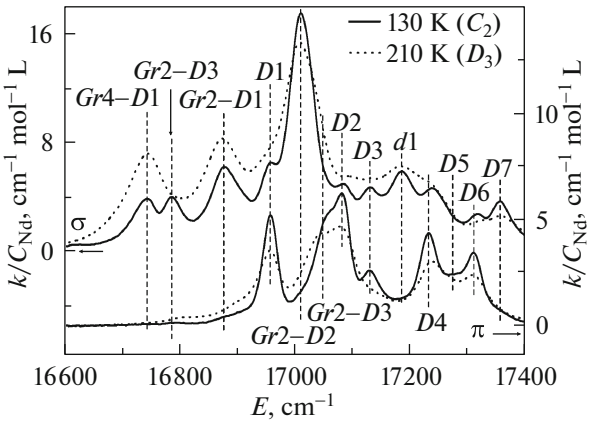

Fig. 7. Optical absorption spectra of the transition $^4I_{9/2} \rightarrow {}^4G_{5/2} + {}^2G_{7/2}$ (D) of Nd^{3+} ions in the π and σ polarizations for the $Ho_{0.75}Nd_{0.25}Fe_3(BO_3)_4$ crystal at T = 130 and 210 K.

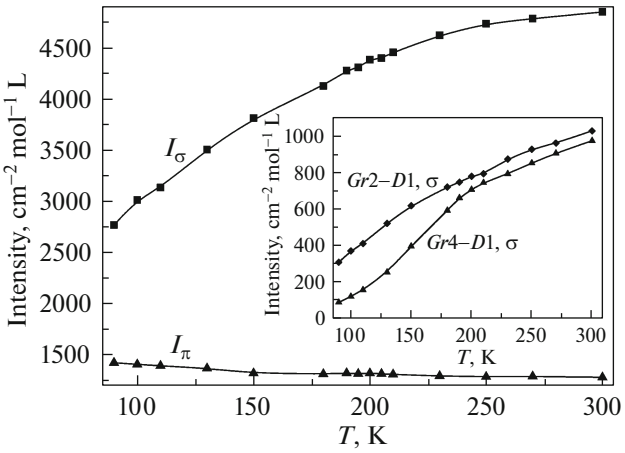

Fig. 8. Temperature dependences of integral intensities of the transition $^4I_{9/2} \rightarrow {}^4G_{5/2} + {}^2G_{7/2}$ (D) of Nd^{3+} ions in the $Ho_{0.75}Nd_{0.25}Fe_3(BO_3)_4$ crystal in the π and σ polarizations. Inset: temperature dependences of the intensity of some lines of the D band.

In the region of transition D, we studied the optical absorption spectra of the $Ho_{0.75}Nd_{0.25}Fe_3(BO_3)_4$ crystal as a function of temperature. Figure 7 shows the π- and σ-polarized spectra at temperatures of 130 and 210 K, respectively, below and above the temperature of the structural transition $P3_121 \rightarrow R32$ (the local symmetry change $C_2 \rightarrow D_3$). Based on the measured optical absorption spectra of the $Ho_{0.75}Nd_{0.25}Fe_3(BO_3)_4$ crystal in the temperature range of 90–300 K, we plotted the temperature dependences of the integral intensities I_π and I_σ of the D transition in Nd^{3+} ions in the π and σ polarizations, respectively (Fig. 8). In the obtained dependences, there are no pronounced features in the region of the structural transition (T = 203 K [15]). However, the different temperature behaviors of the intensity in the π and σ polarizations are indicative of a change in the local environment of the Nd^{3+} ion upon temperature variation, at least, in the excited state.

To determine the temperature dependences of the intensities of individual lines of band D, the obtained spectra were decomposed into Lorentzian components. In the spectra shown in Fig. 7, one should pay attention to the behavior of the two lines, $D3$ and $Gr5$–$D3$. The disappearance of line $D3$ in the π polarization with increasing temperature is related to the change in the local symmetry of Nd^{3+} ions from C_2 to D_3. Line $D3$ is a transition from the lower component of the ground state splitting and its intensity should decrease with increasing temperature. Line $Gr5$–$D3$ is a transition not from the lower component of the ground state splitting and its intensity should increase with temperature, as it happens in the σ polarization with lines $Gr4$–$D1$ and $Gr2$–$D1$ (Fig. 7 and inset in Fig. 8). The disappearance of line $Gr5$–$D3$ in the σ polarization with increasing temperature (Fig. 9) is related to the local symmetry change during the structural transition. The transition $Gr5$–$D3$ becomes forbidden in the D_3 symmetry in the σ polarization. According to the selection rules in the D_3 symmetry (Table 1), this forbiddenness is implemented for the transitions between the $E_{3/2}$ states. Based on Table 2, we may conclude that this is a transition to the $D3$ level. The difference between the energies of lines $D3$ and $Gr5$–$D3$ yields the position of the $Gr5$ level with the $E_{3/2}$ symmetry in group D_3 (Table 2). Line $Gr5$–$D3$ ($E_{3/2}$–$E_{3/2}$), according to the selection rules (Table 1), is allowed also in the π spectra of the $Nd_{0.5}Gd_{0.5}Fe_3(BO_3)_4$ and $NdFe_3(BO_3)_4$ crystals, but is very weak (Fig. 6).

Figure 9 shows the temperature dependence of the intensity of line $D3$ in the π polarization, which decreases both due to a decrease in the population of the $Gr1$ level with increasing temperature and, mainly, due to the local symmetry change from C_2 to D_3. The same figure shows the intensity of line $Gr5$–$D3$ in the σ polarization. In this dependence, the intensity growth caused by an increase in the population of the initial $Gr5$ state with increasing temperature competes with the intensity drop due to the local symmetry change from C_2 to D_3. It can be seen from the temperature dependences of the intensities of lines $D3$ and $Gr5$–$D3$ that they disappear at a temperature of ~200 K, which is in good agreement with the structural transition point obtained in [15].

In addition, we investigated the change in the crystal lattice parameters of the $Ho_{0.75}Nd_{0.25}Fe_3(BO_3)_4$ crystal as a function of temperature (Fig. 10). It turned out that the lattice parameter a changes stepwise at the temperature of the structural transition, which points out the occurrence of a first-order transition. At the same time, the lattice parameter c changes smoothly.

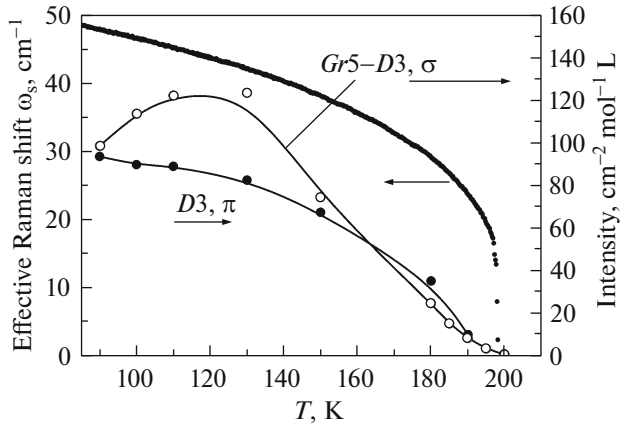

Fig. 9. Temperature dependences of intensities of lines $D3$ and $Gr5–D3$ of the D band of Nd^{3+} ions and positions of the soft structural mode line [15] in the $Ho_{0.75}Nd_{0.25}Fe_3(BO_3)_4$ crystal.

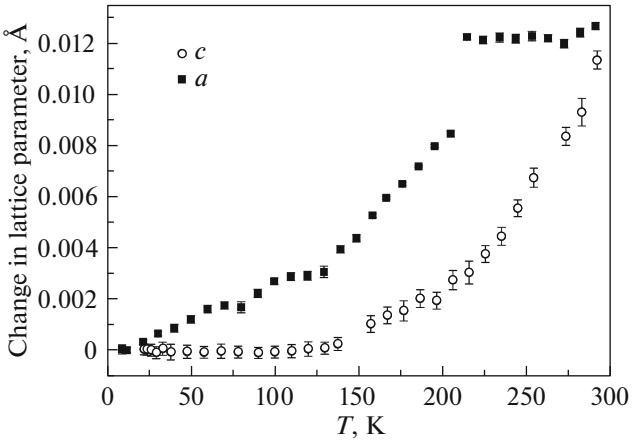

Fig. 10. Temperature dependence of the lattice parameters of the $Ho_{0.75}Nd_{0.25}Fe_3(BO_3)_4$ crystal.

For completeness, Fig. 9 shows the change in the position of the line of a soft structural mode in the $Ho_{0.75}Nd_{0.25}Fe_3(BO_3)_4$ crystal as a function of temperature from [15]. The soft mode position also changes stepwise. Attention is drawn to the fundamental difference between the temperature variations in the structural (lattice and soft mode) parameters and the intensity of absorption lines $f–f$ in the region of the structural transition (Figs. 9, 10). This difference originate from the different nature of the discussed parameters. The structural parameters are mainly related to the even component of the crystal field, while the intensity of the $f–f$ transitions is related entirely to the odd component. It follows from the temperature dependences of the intensity of the $f–f$ transitions shown in Fig. 9 that the odd crystal field component of the lower symmetry does not appear stepwise during the structural transition, but smoothly increases from zero as the temperature decreases from the structural transition point.

4. CONCLUSIONS

The polarized absorption spectra of the Nd^{3+} ion in the $Ho_{0.75}Nd_{0.25}Fe_3(BO_3)_4$ crystal were measured and compared with the spectra of the Nd^{3+} ion in the $Nd_{0.5}Gd_{0.5}Fe_3(BO_3)_4$ and $NdFe_3(BO_3)_4$ crystals at 90 K. Electronic transitions were identified and their energies and intensities were determined. Splittings of the excited electron multiplets of Nd^{3+} ions in a crystal field were established. The difference between multiplet splittings in the investigated crystals suggests the difference between the even crystal field components in the region of the Nd^{3+} ion in these crystals. At 90 K, the integral intensity of a sum of all the transitions in the $Ho_{0.75}Nd_{0.25}Fe_3(BO_3)_4$ crystal is noticeably higher than in the other examined crystals, which points out a larger odd crystal field component, due to which the $f–f$ transitions become allowed.

The absorption spectra of the transition $^4I_{9/2} \rightarrow {}^4G_{5/2} + {}^2G_{7/2}$ in the $Ho_{0.75}Nd_{0.25}Fe_3(BO_3)_4$ crystal were measured as a function of temperature in the range of 90–300 K. In the spectra of this crystal at temperatures below the structural transition point, the lines forbidden in the D_3 symmetry appear due to the lowering of the local symmetry of Nd^{3+} ions. A similar phenomenon is observed in all the investigated absorption bands.

The change in the crystal lattice parameters of the $Ho_{0.75}Nd_{0.25}Fe_3(BO_3)_4$ crystal with temperature was studied. It turned out that the lattice parameter a changes stepwise at the temperature of the structural transition, which suggests the occurrence of a first-order transition. At the same time, the lattice parameter c changes smoothly. The position of a soft structural mode also changes stepwise. The temperature variations in the structural (lattice and soft mode) parameters and the intensities of the $f–f$ absorption lines appearing below the structural transition are fundamentally different. The structural parameters are mainly related to the even crystal field component, while the intensity of the $f–f$ transitions is entirely related to the odd component. According to the obtained temperature dependences of their intensities, the odd crystal field component of the lower symmetry does not appear stepwise during the structural transition, but smoothly increases from zero as the temperature decreases from the structural transition point.

FUNDING

The reported study was funded by Russian Foundation for Basic Research, Government of Krasnoyarsk Territory, Krasnoyarsk Regional Fund of Science, to the research project No. 19-42-240003 “Influence of the local

environment on magneto-optical properties of *f–f* transitions in rare-earth aluminum and iron borates" and the Russian Foundation for Basic Research, project No. 19-02-00034.

This research used resources at the X21 beamline of the National Synchrotron Light Source, a U. S. Department of Energy (DOE) Office of Science User Facility operated for the DOE Office of Science by Brookhaven National Laboratory under Contract No. DE-AC02-98CH10886.

CONFLICT OF INTEREST

The authors declare that they have no conflicts of interest.

REFERENCES

1. A. K. Zvezdin, S. S. Krotov, A. M. Kadomtseva, G. P. Vorob'ev, Yu. F. Popov, A. P. Pyatakov, L. N. Bezmaternykh, and E. A. Popova, JETP Lett. **81**, 272 (2005).
2. A. M. Kadomtseva, Yu. F. Popov, G. P. Vorob'ev, A. P. Pyatakov, S. S. Krotov, K. I. Kamilov, V. Yu. Ivanov, A. A. Mukhin, A. K. Zvezdin, A. M. Kuz'menko, L. N. Bezmaternykh, I. A. Gudim, and V. L. Temerov, Low Temp. Phys. **36**, 511 (2010).
3. A. K. Zvezdin, G. P. Vorob'ev, A. M. Kadomtseva, Yu. F. Popov, A. P. Pyatakov, L. N. Bezmaternykh, A. V. Kuvardin, and E. A. Popova, JETP Lett. **83**, 509 (2006).
4. A. M. Kadomtseva, Yu. F. Popov, G. P. Vorob'ev, A. A. Mukhin, V. Yu. Ivanov, A. M. Kuz'menko, A. S. Prokhorov, L. N. Bezmaternykh, V. L. Temerov, and I. A. Gudim, in *Proceedings of the 21st International Conference on New in Magnetism and Magnetic Materials* (Moscow, 2009), p. 316.
5. G. P. Vorob'ev, Yu. F. Popov, A. M. Kadomtseva, E. V. Kuvardin, A. A. Mukhin, V. Yu. Ivanov, L. N. Bezmaternykh, I. A. Gudim, and V. L. Temerov, in *Proceedings of the 3rd International Symposium on Media with Structured and Magnetic Ordering Multiferroics-3, Rostov-na-Donu, Loo, 2011*, p. 80.
6. D. Jaque, J. Alloys Compd. **323–324**, 204 (2001).
7. A. Brenier, C. Tu, Z. Zhu, and B. Wu, Appl. Phys. Lett. **84**, 2034 (2004).
8. X. Chen, Z. Luo, D. Jaque, J. J. Romero, J. Garcia Sole, Y. Huang, A. Jiang, and C. Tu, J. Phys.: Condens. Matter **13**, 1171 (2001).
9. Y. Saeed, N. Singh, and U. Schwingenschlo, J. Appl. Phys. **110**, 103512 (2011).
10. S. A. Klimin, D. Fausti, A. Meetsma, L. N. Bezmaternikh, P. H. M. van Loosdrecht, and T. T. M. Palstra, Acta Crystallogr. B **61**, 481 (2005).
11. Y. Hinatsu, Y. Doi, K. Ito, M. Wakeshima, and A. Alemi, J. Solid State Chem. **172**, 438 (2003).
12. H. Zhang, S. Liu, C. S. Nelson, L. N. Bezmaternykh, Y.-S. Chen, S. G. Wang, R. P. S. M. Lobo, K. Page, M. Matsuda, D. M. Pajerowski, T. J. Williams, and T. A. Tyson, J. Phys.: Condens. Matter **31**, 505704 (2019).
13. J. C. Joubert, W. B. White, and R. Roy, J. Appl. Crystallogr. **1**, 318 (1968).
14. J. A. Campá, C. Cascales, E. Gutiérrez-Puebla, M. A. Monge, I. Rasines, and C. Ruíz-Valero, Chem. Mater. **9**, 237 (1997).
15. A. S. Krylov, S. N. Sofronova, I. A. Gudim, S. N. Krylova, R. Kumar, and A. N. Vtyurin, J. Adv. Dielectr. **8**, 1850011 (2018).
16. M. N. Popova, E. P. Chukalina, T. N. Stanislavchuk, B. Z. Malkin, A. R. Zakirov, E. Antic-Fidancev, E. A. Popova, L. N. Bezmaternykh, and V. L. Temerov, Phys. Rev. B **75**, 224435 (2007).
17. A. V. Malakhovskii, S. L. Gnatchenko, I. S. Kachur, V. G. Piryatinskaya, A. L. Sukhachev, and V. L. Temerov, J. Magn. Magn. Mater. **401**, 517 (2016).
18. A. V. Malakhovskii, A. L. Sukhachev, A. A. Leont'ev, I. A. Gudim, A. S. Krylov, and A. S. Aleksandrovsky, J. Alloys Compd. **529**, 38 (2012).
19. A. L. Sukhachev, A. V. Malakhovskii, A. S. Aleksandrovsky, I. A. Gudim, and V. L. Temerov, Opt. Mater. **83**, 87 (2018).
20. A. D. Balaev, L. N. Bezmaternykh, I. A. Gudim, V. L. Temerov, S. G. Ovchinnikov, and S. A. Kharlamova, J. Magn. Magn. Mater. **258–259**, 532 (2003).
21. I. A. Gudim, E. V. Eremin, and V. L. Temerov, J. Cryst. Growth **312**, 2427 (2010).

Translated by E. Bondareva